Desalination 608 (2025) 118848

Contents lists available at ScienceDirect

Desalination

journal homepage: www.elsevier.com/locate/desal

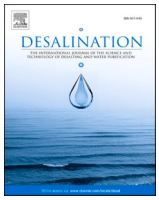

Thermally driven ultrapure water production for water electrolysis – A techno-economic analysis of membrane distillation☆

R. Schwantes [a,*], Y. Morales [b], E. Pomp, J. Singer [b], K. Chavan [c], F. Saravia [b]

[a] Fraunhofer Institute for Solar Energy Systems ISE, Heidenhofstrasse 2, 79110 Freiburg, Germany
[b] DVGW - Research Center at Engler-Bunte-Institut of KIT, Water Chemistry and Water Technology, Engler-Bunte-Ring 9, 76131 Karlsruhe, Germany
[c] Chavan Water Solutions, 79224 Umkirch, Germany

HIGHLIGHTS

- MD module design specifically for integration with electrolyzer waste heat
- Distillate quality experiments yield conductivity under 3 µS/cm
- Comparable RO system design and economic comparison with MD
- MD proves to be more cost efficient than RO when waste heat is available.

ARTICLE INFO

Keywords:
Ultrapure water
Membrane distillation
Electrolysis
Heat coupling
Techno-economic evaluation

ABSTRACT

The transition to hydrogen production with renewable energies necessitates ultrapure water (UPW) as a raw material for water electrolysis, which imposes stringent quality and economic demands on water treatment technologies. This study evaluates the techno-economic feasibility of membrane distillation (MD) as an alternative to reverse osmosis (RO) for UPW production. Utilizing waste heat from a 5 MW proton exchange membrane (PEM) electrolyzer, which would otherwise require active cooling to sustain operation of the electrolyzer, the proposed MD system employs permeate gap membrane distillation to treat feedwaters with brackish and seawater salinities (i.e., 5 g NaCl /kg and 34.3 g NaCl/kg, respectively). The study incorporates numerical simulations to analyse system design parameters and energy consumption of MD and RO systems designed to produce 1 t/h of distillate, as well as experimental data on distillate water quality. Results demonstrate that MD systems achieve high-quality distillate (<3 µS/cm) under the tested salinities and at competitive costs. Estimated unit costs per ton of produced distillate for MD range from €2.33 to €2.85 for either brackish or seawater feed at electricity prices of €0.10–€0.40/kWh, while RO costs range from €2.80 to €5.51 under comparable conditions. The presented annual costs also reflect the cost advantage, especially for seawater desalination with MD costs, approx. 40 % lower than RO. MD shows advantages in energy efficiency with thermal energy provided as low-grade heat. This work shows that MD can be a cost- efficient and versatile solution for UPW production powered by PEM electrolyzer waste heat.

1. Introduction

Producing hydrogen (H_2) by use of renewable energies has become a priority on the political agenda of many countries as it provides a potential alternative energy resource, storage and a valuable compound for chemical processing to fossil fuels [1]. The required amount of highly pure water and its relatively energy intensive production, however, is not so much a part of the mainstream awareness. Nonetheless, it can by no means be neglected and must be fully considered as a raw material necessary for operation of a hydrogen electrolysis system [2]. Since the direct use of seawater poses several crucial challenges [3], the required water that is fed to today's commercially available electrolyzers must be free of salts, colloids and organic compounds to prevent deterioration and performance losses of the cells [4–8]. Electrolyzer providers commonly define water quality requirements based on standards such as

☆ This article is part of a Special issue entitled: 'Ultrapure Water' published in Desalination.

* Corresponding author.
E-mail address: rebecca.schwantes-chavan@ise.fraunhofer.de (R. Schwantes).

https://doi.org/10.1016/j.desal.2025.118848
Received 23 December 2024; Received in revised form 24 March 2025; Accepted 25 March 2025
Available online 26 March 2025

Nomenclature

A	membrane area [m^2]
A_{tot}	Total system membrane area [m^2]
a_{amor}	annual amortization costs [Eur/a]
a_{chem}	annual chemical costs [Eur/a]
a_{el}	annual costs for electricity [Eur/a]
a_{in}	annual insurance costs [Eur/a]
a_l	annual labor costs [Eur/a]
a_{rep}	annual replacement costs [Eur/a]
a_{SM}	annual service and maintenance costs [Eur/a]
AGMD	air gap membrane distillation
C_I	total capital investment costs [Eur]
C_{MOD}	module costs [Eur]
C_{ROP}	rest of plant costs [Eur]
CAPEX	capital expenditures
c_P	specific heat capacity [kJ/kgK]
d_M	nominal pore diameter membrane[µm]
F_c	flow rate condenser channel [kg/h]
F_e	flow rate evaporator channel [kg/h]
GOR	gained output ratio [−]
H	total head for centrifugal pump [m]
h	height of active membrane area [m]
Δh_v	heat of evaporation of water [kJ/kg]
H_2	hydrogen
i	interest rate
$\dot{j}_d$	distillate transmembrane flux [kg/m^2h]
k	number of modules [−]
L	channel length [m]
$\dot{m}_d$	distillate output per module [kg/h]
$\dot{m}_f$	feed mass flow rate [kg/h]
MD	membrane distillation
n	lifetime
OPEX	operating expenditures
P_{el}	electric power [kW]
p_{el}	price of electricity power [Eur/kWh]
PEM	proton exchange membrane
PGMD	permeate gap membrane distillation
$\dot{q}_{aim}$	aimed distillate capacity of MD system
$\dot{q}_d$	distillate capacity of MD system
RO	reverse osmosis
ROI	return on invest
S_{ci}	condenser inlet salinity [g/kg]
S_{eo}	evaporator outlet salinity [g/kg]
SEC_{el}	electric specific energy consumption [kWh/m^3]
SEC_{th}	thermal specific energy consumption [kWh/m^3]
SWRO	sea water reverse osmosis
T	temperature [°C]
T_{ci}	condenser inlet temperature [°C]
T_{co}	condenser outlet temperature [°C]
T_{ei}	evaporator inlet temperature [°C]
T_{eo}	evaporator outlet temperature [°C]
T_m	mean temperature [°C]
UPW	ultra pure water
V	voltage [V]
V_{rev}	reversible voltage [V]
$x_{\%}$	percental deviance [%]
y	replacement [−]
z	number of exchanged electrons
δ_B	backing thickness [µm]
δ_F	foil thickness [µm]
δ_M	membrane thickness [µm]
δ_{PG}	permeat gap thickness [µm]
$\delta_{E/C}$	evaporator and condenser channel thickness [µm]
ϵ_B	backing porosity [−]
ϵ_M	membrane porosity [−]
ϵ_P	efficiency of pump [%]
ϵ_S	spacer porosity [−]
ρ	density [g/L]
τ_M	membrane tortuosity [−]
Δh_v	enthalpy difference [kJ/mol]
ΔT	temperature difference [K]

those provided by the American Society for Testing and Materials (ASTM). Typically, water must comply with different limits including electrical conductivities of <5 µS/cm or even <0,1 µS/cm, corresponding to quality types IV and I by the ASTM D1193-06 standards [9]. To maintain such high qualities, ultrapure water (UPW) or pure water (PW) must be either provided directly to the electrolyzer plant or produced onsite. Desalination is a viable option but should be implemented in concordance with a sustainable management of natural resources [10,11], for example by using wind and solar power or waste heat as an energy source. At the same time, electrolyzers require cooling, providing the possibility of low-grade heat coupling to a thermal water production process such as membrane distillation.

The production of UPW is commonly conducted by a combination of several processes. Depending on the feed water quality, pretreatment through coagulation, flocculation and filtration removes suspended solids from the feed water after which it is then further treated by a desalination process to remove salts, organics and colloid particles [5]. In the final step, the water is polished e.g. using deionization, degasification, and ultraviolet treatment to meet the required quality. The desalination step plays a significant role in the process chain, as its task is to reject the majority of impurities [12]. Typically, membrane technologies such as reverse osmosis (RO) and electrodialysis (ED) are used. If thermal energy is available, thermal processes such as multistage flash or multi-effect distillation can be applied instead [13]. RO is the most widely applied membrane desalination technology but comes with certain drawbacks. Seawater reverse osmosis (SWRO) requires high pressures of up to 60 bar or more moderate feed pressures of 10–15 bar when desalinating brackish water. In both cases intensive pretreatment such as chlorination/dechlorination and dosage of antiscalants is needed for the removal of dispersed particles. SWRO systems with a recovery rate between 40 and 60 % create a highly concentrated brine as a side product. When disposed to the sea, higher salinity seawater has a significant environmental impact putting osmotic stress on local marine wildlife [14].

In recent decades, alternative desalination technologies such as membrane distillation have been developed, gaining relevance in the research and start-up sector due to their ability to produce high-quality water from saline and other feed sources [15–19] as well as its implementation for other recovery and extraction applications [20,21]. One advantage is the relatively low operating temperature level of the process, which allows the coupling with low-grade energy sources [22] as well as its ability to operate under dynamic operation conditions. In comparison to RO the feed in membrane distillation can be circulated with conventional centrifugal pumps, while RO systems require high pressure pumps to reach feed pressures of 10–15 bar in case of brackish water and up to 60 bar in case of seawater reverse osmosis (SWRO) [14,23]. A further advantage of membrane distillation over RO in certain applications is that pretreatment steps such as chlorination/dichlorination, dosage of antiscalants and acid addition are not as necessary.

Comprehensive work and reporting on MD as an alternative membrane process to RO for PW production is limited [24–26]. Reports including a specific MD module design and a techno-economic comparison with RO are lacking. The possibility of producing UPW from drinking water with membrane distillation test setup has however been show and distillate conductivities with <0.8 μS/cm have been previously achieved [27] making a target of <5 μS/cm even with varying feed solutions a realistic scenario. A pilot scale system consisting of a 50 kW_e PEM-electrolyzer stack with an integrated MD system was tested for over seven weeks by [28] using sea water as feed for the MD system. The authors were able to cool the electrolyzer and simultaneously produce almost three times the required distillate with the excess heat of the electrolyzer. It was estimated that integrated, heat coupled MD-PEM systems need to be of large scale (>100 $kg\,H_2/h$) to be cost-effective [29]. Investigations by [6] concluded that MD systems can produce distillate from electrolyzers excess heat at a lower price than RO. Nonetheless, further implementation and full-scale application-oriented investigations of theoretical and practical nature are required to further pinpoint the exact potential of MD in conjunction with integrated PW production for water electrolysis.

It must be noted that MD systems in general require further development with respect to cost-effective operation on a larger scale and a complete commercial breakthrough of membrane distillation as a fully accepted industrial technology has not been achieved so far [30]. Several enterprises committed to the commercialization of MD exist [31,32], but one of the main barriers to market besides as the lack of cost efficient and specifically designed membrane materials that prevents MD from being a fully established solution in the industrial water treatment state-of-the-art is the cost-effective supply of sufficient thermal energy to power the process. With the relative abundance of waste heat available, producing UPW for hydrogen electrolysis could potentially be the long-awaited break through application for MD.

The following work evaluates the potential of membrane distillation as a viable, cost- and energy-effective alternative technology to RO to produce UPW for PEM electrolyzers. Besides an initial experimental presentation on the long-term achievable distillate quality conducted in a small-scale set-up, a specific full-scale MD module design is presented alongside a suggested strategy for the thermal integration of the MD system into a PEM electrolyser unit. Two different types of feed water sources are considered, a low salinity of 5 gNaCl/kg, representing feed sources up to the salinity of brackish water and a higher salinity of 34,3 gNaCl/kg representing that of seawater. The work furthermore proposes an MD-system design, producing enough distillate to feed a 5 MW_{el} PEM electrolyzer, estimated to be 1 t/h of distillate. A fully validated simulation tool is used to conduct a performance analysis of the MD-modules and select the most beneficial channel length for the operation with waste heat, before comparing the concept to an equivalent RO system techno-economically.

2. MD fundamentals

2.1. Membrane distillation process

Membrane distillation is a thermal separation process based on a vapour pressure difference as driving force across a hydrophobic, highly porous membrane. This vapour pressure difference between either side of the membrane drives liquid particles to change phase and pass through the membrane in gaseous form [33]. MD has the advantage of utilizing low-temperature heat sources of <90 °C and operating at ambient pressure. In comparison to RO, the membrane can be produced from a higher variety of chemically resistant and hydrophobic materials with pore sizes ranging from 0.05 to 0.4 μm. Having relatively large pores in comparison to diffusive pathways of RO, fouling has a lower impact. MD has been thoroughly investigated and trialed for desalination purposes in pilot scale units for on- and offshore cases [34–36]. Furthermore, the details of heat and mass transport phenomena in MD have been provided in a wide range of publications [23,33,37–39] and can be considered well investigated fundamentally. The driving force for vapour transfer through a hydrophobic, porous membrane can be applied in a variety of different ways; by an osmotic pressure difference [40], an absolute pressure difference [41] or a temperature difference. All result in a difference in vapour pressure across the membrane and evoke a mass flux.

Within the thermally driven process variants, several sub-variants of heat utilization and heat recovery can be implemented. With relevance to this work, Fig. 1 shows two typical basic configurations.

The simplest variant is Direct Contact Membrane Distillation (DCMD) in which a warmer feed stream is separated from a cooler permeate stream via the membrane. Although it provides a very high heat utilization and low thermal resistance for heat transfer, it suffers from a set of drawbacks such as added complexity in the design of the surrounding system as well as a higher risk of permeate contamination in the event of leakages. Heat recovery in DCMD is only possible with additional heat exchangers and requires two main pumps instead of one. Thus, it is not commonly implemented on a larger scale. Permeate Gap Membrane Distillation (PGMD) on the other hand, is an adapted version of DCMD. A third channel, called the permeate gap, is introduced between the hot and cold channel. It is separated from the cooling channel by an impermeable foil. This provides the advantage of separating the permeate from the cooling liquid and thus enabling internal heat recovery inside the module. The feed can thereby be used as both the heating and cooling flow simultaneously [23,34]. The additional film and the distillate filled channel add to the thermal resistance in the PGMD variant, but with a low overall impact on the process. Vacuum can be applied in MD in several different ways but comes with reduced membrane lifetime and permeate quality [42,43] and require additional electrically powered system components and added system complexity.

For the application analyzed in this work, feed solutions with low TDS - brackish water- as well as higher TDS, namely seawater, are considered. For the investigated salinity range of feed solutions, it has been well presented previously that PGMD is the most efficient variant of MD besides DCMD if the goal is a robust solution without the application of vacuum [23] and will thus be selected for the application presented within this work.

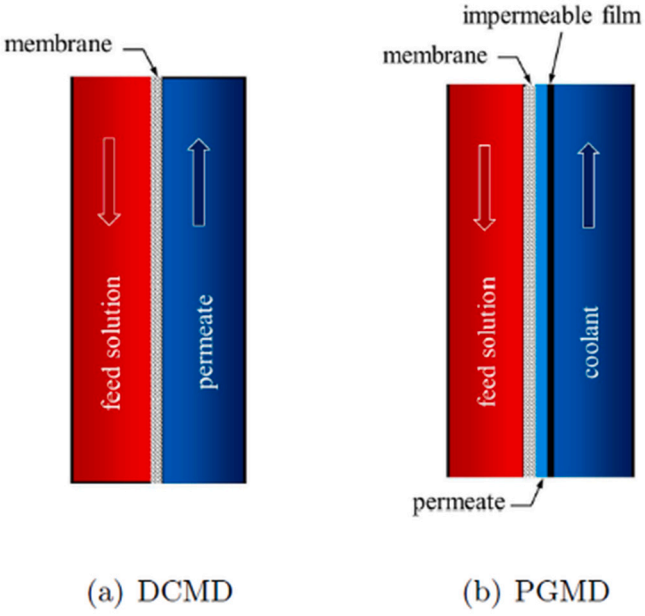

Fig. 1. Basic thermal- powered MD configurations a) DCMD, b) PGMD [23].

2.2. Membrane distillation basic equations

This section describes the key performance indicators of membrane distillation, the assumed available heat from PEM electrolysers, the sensitivity analysis for the plant design and the flux and water quality experiments. The key performance indicators (KPI) of MD modules will be introduced in the following equations. They will be used to evaluate the results of an MD system design parametric study.

The output of a module $\dot{m}_d$ is defined by the mass of distillate produced per hour.

$$\dot{m}_d \left[\frac{kg}{h}\right] \tag{1}$$

Transmembrane flux is the rate of distillate production per membrane area:

$$j_d = \frac{\dot{m}_d}{A} \left[\frac{kg}{(m^2 h)}\right] \tag{2}$$

Next, in Eq. (3) gained output ratio (GOR) is introduced. GOR gives an indication of the quality of the internal heat recovery by putting the heat required for phase change of the liquid molecules into relation with heat supplied to the system externally. The larger the GOR, the more efficient the heat recovery of the MD-system.

$$GOR = \frac{\dot{m}_d \Delta h_v}{\dot{m}_f c_p (T_{ei} - T_{co})} [-] \tag{3}$$

Hereby, $\dot{m}_f$ is the mass flow rate of the feed solution and c_p its temperature-dependent specific heat capacity. The condenser outlet and evaporator inlet temperatures T_{co}, T_{ei} are indicated in Fig. 3. The specific thermal energy consumption SEC_{th} calculated in Eq. 4 describes the required heat that is needed to produce one ton of distillate.

$$SEC_{th} = \frac{\Delta h_v}{GOR} \left[\frac{kWh}{t}\right] \tag{4}$$

The electric energy needed to power the centrifugal pumps of an MD system is characterized by the specific electrical energy consumption SEC_{el} in Eq. (5). It is the electrical energy consumed for every ton of produced distillate.

$$SEC_{el} = \frac{P_{el}}{\dot{m}_d} \left[\frac{kWh}{t}\right] \tag{5}$$

Electrical power P_{el} is calculated from the required hydraulic power divided by the efficiency of the pumps. The hydraulic power that must be overcome is dependent on pressure losses created by heat exchangers, pipes, and MD-module channel resistance. Pressure losses of MD-modules have previously been experimentally evaluated for channel thicknesses between 2 and 3.2 mm and channel lengths of 3.5 to 10 m [23].

The estimation for the electrical power consumption P_{el} of the circulation pump (centrifugal) with an assumed efficiency (ϵ_P) of 0.75 is carried out according to Eq. (6) [44] using the total mass circulation flow in the condenser and evaporator channels for the MD (F_e), the total head for the centrifugal pump (H) and the acceleration due to gravity (g).

$$P_{el-MD} = \frac{(F_e\, g\, H)}{(3.6\, 10^6) \in_p} \tag{6}$$

The evaporator outlet salinities S_{eo} of the concentrated retentate is approximated by Eq. 7 neglecting the salinity in the distillate and only considering the salinity of the feed inlet.

$$S_{eo} = \frac{\dot{m}_f\, S_f}{\left(\dot{m}_f - \dot{m}_d\right)} \left[\frac{g}{kg}\right] \tag{7}$$

$$T_{m=} \frac{(T_{ei} - T_{co})}{2} [^{\circ} C] \tag{8}$$

Eq. (8) describes the calculation of the mean process temperature T_m, required for the characterisation of experimentational results in Section 4.

$$RR_{=} \frac{\dot{m}_d}{\dot{m}_f} \times 100\ [\%] \tag{9}$$

Recovery ratio RR, given in Eq. (9) is an indicator of the percentage of mass flow of distillate produced from a certain feed mass flow.

3. Experimental evaluation of MD distillate quality

3.1. Laboratory system set-up

A series of experiments were conducted to assess the distillate quality over more than 120h of operation using the same membrane material, condensation foil and spacers as in the module analysis presented in Section 5. The experiments were performed in an automated laboratory scale PGMD setup. A schematic of the setup is shown in Fig. 2. The setup consists of an evaporator (feed) and a condenser loop that flow through a flat-sheet MD cell. Temperature and flow rates are controlled automatically in the two separate loops. During the experiments, the temperature difference across the membrane was adjusted based on the temperatures at the inlet of the evaporator T_{ei} and the outlet of the condensator T_{co} shown in Fig. 2. Produced distillate is collected through a separate line in which electrical conductivity and temperature are recorded continuously and collected in a distillate tank placed on a weighing scale. To ensure constant salinities in the evaporator loop, distillate is periodically pumped back to the evaporator vessel. In Table 1 a list of sensors and components relevant to the laboratory setup is given, including the name of the component and its respective accuracy.

3.2. Experimental conditions

The selected materials for the experimental assessment were defined to represent the components used in the numerical simulations of the MD system. The varied operational parameters were mean temperature T_m, driving force temperature difference ΔT and salinity S_f. Each experiment was started at the highest mean temperature T_m of 56 °C and run for at least 60 h, followed by another period at a T_m of 25 °C for the equal time duration. These variations were performed to represent the conditions of two different mean temperature profile zones which would typically occur in the hotter and the cooler region of a MD module. During startup and after changing temperature settings, the MD setup took several minutes to reach the defined evaporator and condensator temperature levels. To prevent inaccuracies in the calculation of flux and electrical conductivity of the distillate, the first 2 h of generated data after startup or change of temperature were eliminated from the evaluation. The subsequent hourly values were then used to estimate the mean flux and electrical conductivity. In addition to the online conductivity measurements, permeate samples were taken during the experiments to determine the sodium concentration with inductively coupled plasma optical emission spectroscopy (ICP-OES, Agilent 5110). Table 2 summarizes all experimental parameters studied.

Feed solutions were prepared for each experiment in 20L of demineralized water. NaCl (VWR chemicals, ≥99.5 %) was mixed depending on the aimed salinity solutions. Additionally, 20 mg/L sodium azide (Merck, ≥99.0 %) were added to the feed solution to prevent biological growth.

3.3. MD distillate quality results

The experimental results of flux and distillate conductivity were

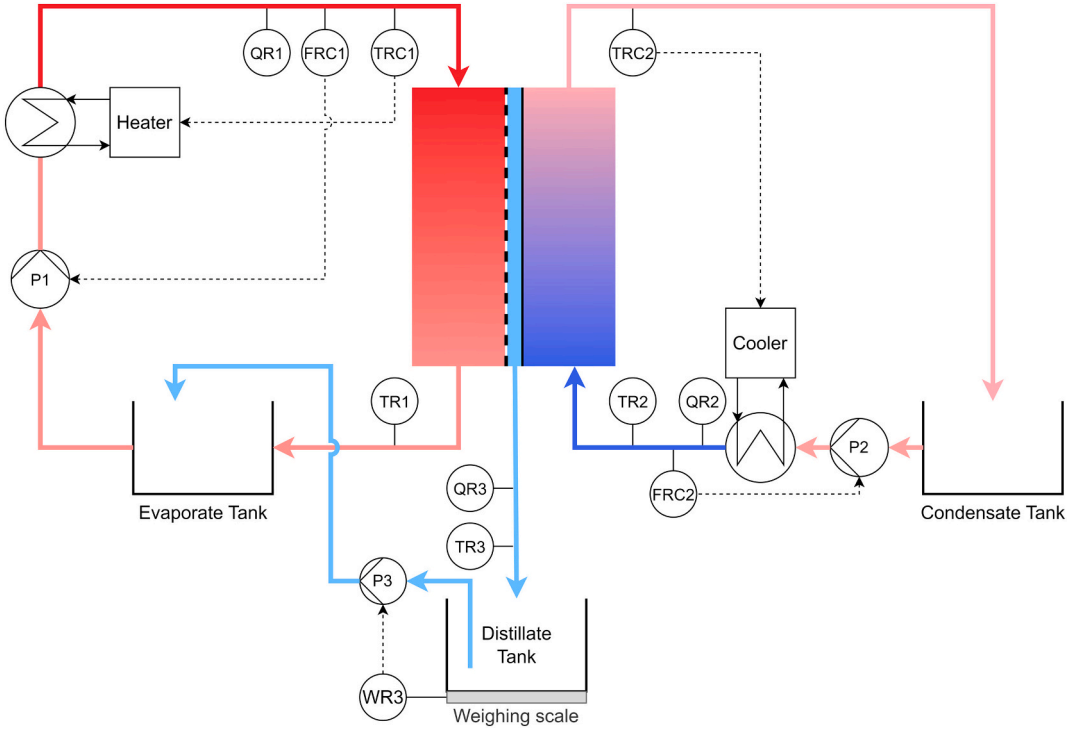

Fig. 2. Schematic of the PGMD lab test cell setup. Evaporator and condenser channels are controlled independently from each other. Mean temperature and temperature difference across the membrane are set by T_{ei} and T_{co}. Flow rates are regulated by F_e and F_c.

Table 1
List of sensors and actors of the laboratory PGMD test cell setup.

Component	Producer	Type	Accuracy/ Range	Name in Fig. 3
Conductivity meters feed	Bürkert	8228	± (0.002 × measured value +5 µS/cm)	QR1, QR2
Conductivity meter distillate	Jumo	BlackLine CR-EC, K = 0.1	±2 %; 0.1µS/cm–1mS/cm	QR3
Volume flow meter	Krohne	OPTIFLUX 4000	± 0.3 % of measured value	FRC1, FRC2
Temperature sensors	TC direct	Pt100	± (0.15 + 0.002 × t)	TRC1, TRC2, TR1, TR2, TR3
Balance distillate	Soehnle	Table balance	±1 g; 0–32 kg	WR3
Pumps	Pentair	Shurflo 2088		P1, P2
Pump distillate	Boxer	3MD		P3
Cooler	Huber	Unichiller 025-H	±2 %	Cooler

Table 2
Experimental parameters for flux PGMD flux analysis.

Parameter	Symbol	Value / type	Unit
Mean temperature	T_m	25; 56	°C
Temperature difference	ΔT	4; 8	K
Feed flow velocity	v_f	0.097	m/s
Feed mass flow rate	$\dot{m}_f$	300	kg/h
Salinity feed	S_f	5; 35.34	gNaCl/kg
Membrane type	–	0.2 Donaldson 6502	µm
Evaporator & Condenser channel spacer thickness	$d_{E/C}$	2.15	mm
Permeate gap spacer thickness	d_{PG}	0.3	mm
Impermeable foil thickness	–	100	µm
Active membrane area	A	387.5	cm^2

monitored in the laboratory setup and are shown in Table 3 for the different operational parameters. The results demonstrate that MD was able to maintain a constant distillate production as well as deliver high purity distillate (<3 µS/cm) under all tested conditions, regardless of variations in feed salinity, mean temperature or temperature difference.

Only slight differences in conductivity were observed between the different mean temperatures. This indicates that comparable qualities may be expected along the length of a theoretical full-scale MD module for the range of salinity tested, even when different temperature zones (e.g. 56 °C and 25 °C) are present. At a feed salinity of 34.3 gNaCl/kg, the distillate conductivity was slightly elevated compared to 5 gNaCl/kg. This difference can be explained by the lower distillate fluxes recorded, which can lead to higher relative impact of micro- leakages of salt into the distillate channel. In conclusion, such slight variations may be affected by different factors during measurements and would not be significant for the electrolysis operation, considering that subsequent polishing steps are implemented after MD and the temperature difference would possibly be even higher than 8 K. Furthermore, the electrical conductivity measurements performed manually confirmed the values recorded in the setup. All analyzed samples showed sodium concentrations below the limit of quantification (0.1 mg/L) of the ICP-OES apparatus. Thus, the results confirm the suitability of PGMD to produce high purity water for a range of feed source salinities from brackish water to seawater.

4. System design and performance analysis for integration with PEM electrolysis

4.1. Integrated MD system design

In the following section, a MD system capacity is designed to feed a 5 MW_{el} PEM electrolyzer stack cell at full load. To account for on- and offshore cases, two different feed water solutions are considered

Table 3
Mean distillate electrical conductivity and flux results from lab-scale PGMD experiments at different feed water salinities, mean temperatures and driving force temperature differences.

		ΔT = 8 K				ΔT = 4 K			
Parameter		Brackish (5 gNaCl/kg)		Seawater (34.3 gNaCl/kg)		Brackish (5 gNaCl/kg)		Seawater (34.3 gNaCl/kg)	
Mean temperature	°C	56	25	56	25	56	25	56	25
Mean distillate cond.	µS/cm	0.5	0.5	2.6	1.1	0.8	0.7	2.1	2.6
		±0.1	±0.1	±0.6	±0.2	±0.1	±0.1	±0.05	±0.2
Flux	kg/m^{2}h	2.48	1.2	1.71	0.88	1.03	0.69	0.66	0,25
		±0.04	±0.09	±0.07	±0.02	±0.29	±0.09	±0.16	±0.02

resembling brackish water and seawater. AirLiquide's 20 MW_{el} PEM plant, which consists of four 5 MW_{el} cell stacks, produces 8.2 t of H_2 per day at 24 full load hours [45]. Assuming 10 kg of UPW for each kg of H_2, one kilogram more than the stoichiometric electrolysis reaction of water, this translates to 0.85 t/h of UPW that is required by a 5 MW_{el} cell stack. The targeted capacity of the MD system is thus selected at a conservatively higher value of 1 ton of distillate per hour.

To maintain a constant temperature in the electrolyzer cell stack, the system must be cooled continuously during operation. An energy and exergy analysis of a PEM electrolyzer plant was performed in [47]. The results showed that the excess heat generated by irreversibilities is much greater than the required heat for the reaction. Depending on the current density at the electrodes, excess heat between 100 and 120 kJ per mol of produced hydrogen is thermodynamically available [47]. The excess heat can be extracted from three sources; from the oxygen stream, the hydrogen stream, or the water recirculation stream using external heat exchangers [48–50]. Alternatively, the cooling fluid can be passed directly along the bipolar plates cooling the cell stack internally [51].

Fig. 3 provides a schematic design of a heat coupled MD-Electrolysis system in which the heat is extracted from the oxygen stream before entering the electrolyzer stack. However, not all the excess heat can be extracted from the system. To account for realistic heat utilization, a heat recovery efficiency of 80 % for an external cooling of the stack and a maximum electric efficiency of 80 % will be assumed as suggested by [48], meaning that 20 % of the electric energy to the stack results in heat. The amount of available heat can be higher (up to around 40 % of the electric energy) depending on operating temperatures and cell pressure [52]. For later discussion in this study, an overall efficiency of 20 % in the PEM system was selected, resulting in 1 MW of available heat at full operation capacity.

Furthermore, the available temperature level of the available heat must be considered. State of the art PEM electrolyzers report operating temperatures of 50 °C–80 °C. As suggested by [48] an available temperature level of 65 °C will be assumed for this work. For this study and as a simplification, dynamics and temperature changes of the available waste heat are not considered. Investigations on the effects of intermittent and variable waste-heat supply to MD systems can be found for example with [53]. Conservatively, a further maximum loss of ΔT of 5 K

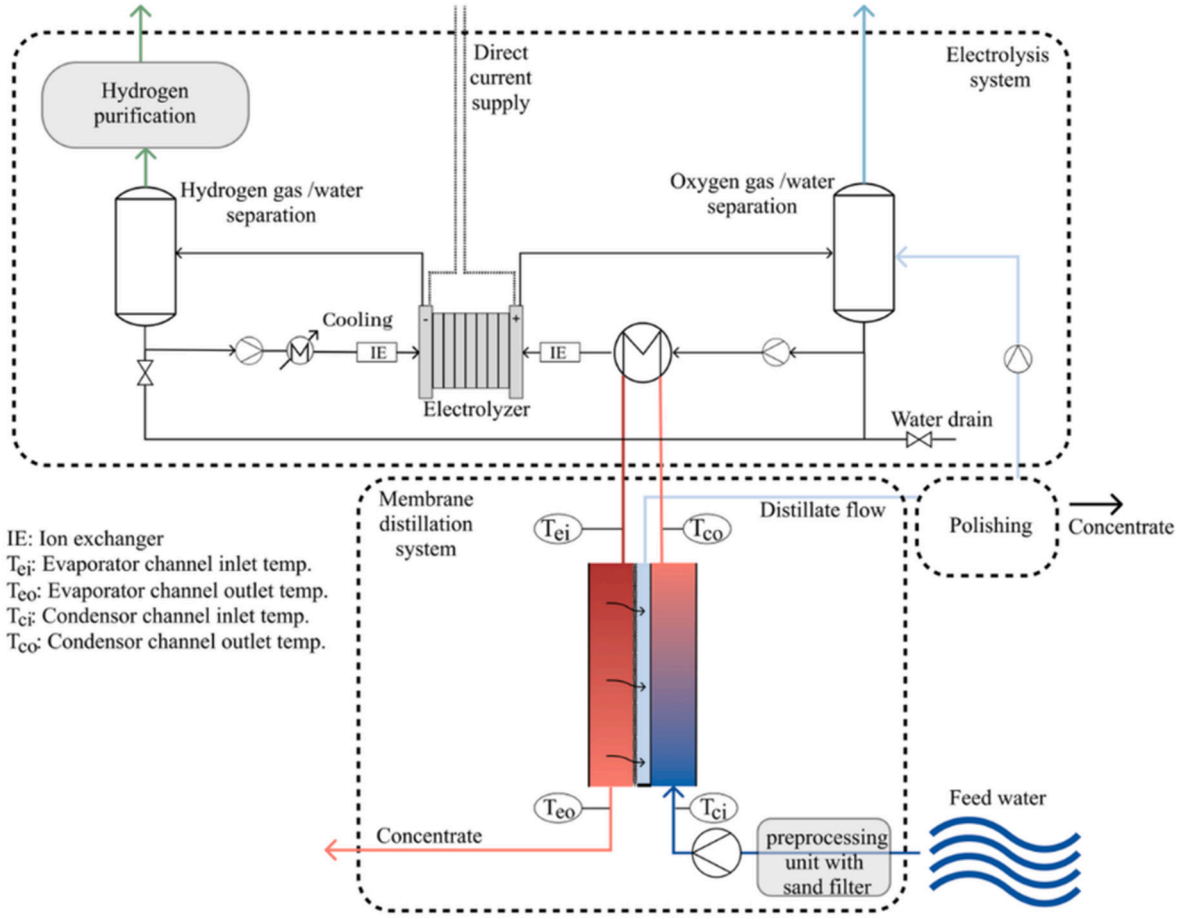

Fig. 3. Schematic of a heat-coupled MD- Electrolysis system based on Emonts et al. [46]. For visual simplification the heat is only transferred by one heat exchanger.

will be considered across the heat exchangers and piping. Based on these assumptions, the temperature of the water entering the evaporator channel of the MD module (T_{ei}) will be considered as 60 °C in all further evaluations.

A performance analysis of the MD system for the scenario shown in Fig. 3 was carried out based on the results of a parametric study with a numerical multi-node simulation tool developed by the Fraunhofer Institute ISE in Freiburg, Germany. The model has been validated for feed concentrations within a range of ~0–120 g/kg of sea salt and NaCl with lab and pilot scale experiments for different channel configurations and lengths and a variety of operational parameters [23,36].

The following KPIs from the simulation were used for the evaluation of the MD system performance:

1. Output and GOR
2. Electrical and thermal specific energy consumption and required membrane area for different channel lengths
3. Discharge concentration and outlet temperature of the concentrate impacting the environment
4. Unit cost of treatment per ton of distillate

Based on the performance analysis of the presented indicators, a selection of channel length and mass flow rates will be made. These selections will then define the installed module membrane area and thermal and electrical energy demand which influences costs. Performance also depends on the environmental conditions such as temperature and feed salinity. The impact of the feed inlet water temperature will be presented at 5, 10 and 20 $^{\circ}C$. The North Sea for example has a temperature of 5–9 °C in winter and 12–17 °C in the summer months [54]. In addition, two salinities of feed water are analyzed. The lower salinity feed 5 gNaCl/kg solution will stand representative for all feed sources with below or in this salinity range such as brackish surface or groundwaters. The other salinity represents seawater at 34.3 gNaCl/kg of solution. A list of parameters and variables as input for the simulation is provided in table in Appendix A. All equations and a full and detailed description of the model is provided by [23].

4.2. MD performance analysis

The following section presents the result analysis of 180 numerically simulated data sets based on the design provided in Fig. 3. The goal of the analysis is the determination of the most cost-effective heat recovery concept for coupling a MD system to a PEM hydrogen electrolyzer. For the given flow channel geometries and feed solutions considered in this work, a channel length of 7 m has repeatedly been identified as a good balance between productivity and efficiency [30,36] for seawater desalination. Thus, to establish a general understanding of the MD-module performance, the first analysis presented in Fig. 4 is of GOR and output per MD module channel for a module channel length of 7 m. Feed mass flow is varied from 100 to 400 kg/h. Since the impact of evaporator temperature is well studied [55–57], the effect of varying condenser inlet temperature T_{ci} is shown here, representing an assumption of different feedwater inlet.

As mentioned, the evaporator inlet temperature T_{ei} is fixed at 60 °C corresponding to the assumed available temperature level coming from the electrolyzer. The results in Fig. 4 show the overall characteristic pattern of increase in distillate output alongside a decrease in GOR for increasing feed mass flow rates in MD modules. Distillate output values per module range from 2.6 to 4.4 kg/h at a feed mass flow of 100 kg/h and 12.5–16.9 kg/h at 400 kg/h. Inversely, GOR values range from around 6–9 at 100 kg/h and decrease to 3.2 and 2.5 at 400 kg/h feed mass flow. This well studied phenomenon [58] of the trade- off between heat recovery and productivity does not change fundamentally under variation of the cold side inlet temperature. In fact, the difference in distillate output between 5 and 10 °C inlet temperature is almost negligible (4–5 %) for both brackish and seawater with a slightly larger

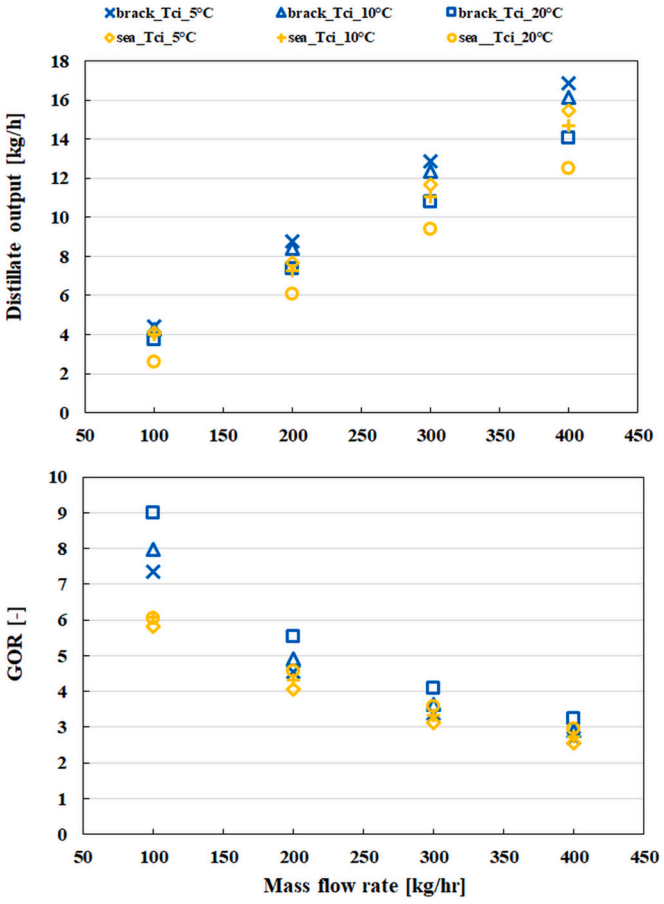

Fig. 4. MD module channel output (top) and GOR (bottom) for a channel length of 7 m with increasing mass flow rates and different feed inlet temperatures r $\dot{m}_f$= 300 kg/h, T_{ei}. = 60 °C; Sal = 0.5 (brack) and 34.3. gNaCl/kg solution (sea).

impact for feed inlet temperatures of 10–20 °C of about 12–13 % for brackish and 15–17 % for seawater. Regarding GOR, values differ by 4–8 % for the inlet temperature range from 5 to 20 °C for seawater. For brackish water the GOR spread is slightly higher at 7–11 %.

The reason for the small to moderate impact of cold side inlet temperature variation between 5 and 20 °C on the KPIs lies in the nature of the inclination of the vapour pressure curve; specifically, its lower inclination in the temperature range for the feed inlet salinities selected in this work. This results in a lower effect on the vapour pressure difference across the membrane (i.e., driving force) compared to the temperatures on the hot side, which are significantly more impactful [23,59,60].

The selection of the range of mass flow rate is another factor which influences the CAPEX and the OPEX in the form of required membrane area or higher thermal energy. Generally, a selection must be based on the availability of waste heat, cost of surface area to install the plant on, maximum desired pressure drop inside the flow channels and cost of electrical energy for pumping. Following a conservative approach, a selection of 300 kg/h feed mass flow rate and 10 °C cold side inlet temperature will be made for the subsequent analyses of the impact of said channel length, as shown in Fig. 4, a 300 kg/h flow rate provides a moderate output at an acceptable GOR. However, it is noteworthy that MD-can be operated dynamically at variable mass flow rates, providing a certain flexibility within the design.

If waste heat is available in an abundant amount, as in the scenario this work is based upon, OPEX caused by thermal heat demand is negligible. Thus, selecting a channel length with <7 m becomes a

potentially more cost-efficient solution, without the need for such high internal heat recovery inside the module. The MD module's channel length determines the surface area and residence time for heat exchange. Fig. 5 allows the analysis of GOR and output for different channel lengths and the salinities of 5 and 34.3 gNaCl/kg solution (brack, sea). An almost linear increase in GOR can be observed for increasing channel length, from ~0.6 at 1 m to 4.6 for brackish water and 4.1 for seawater at 9 m. This is owed to the successively improving internal heat recovery according to the laws of counter current heat exchange. With a larger surface available the internal exchange of heat is higher. The more heat is reused internally, the lower the required external thermal energy supply. Driving force delta T across the membrane decreases with a longer channel and thus the driving force vapour pressure difference - so do the coefficients of mass transfer through the membrane. With increasing salinity, the vapour pressure of the feed is lowered, and the effective driving force vapour pressure difference is reduced. Hereby, the fraction of sensible heat transfer increases compared to the fraction of latent heat, leading to a relative reduction in output and subsequently GOR [30,58].

The distillate output results show this phenomenon even more clearly, with lower output values for the seawater feed across all channel lengths, despite identical operational parameters. Overall, output values increase sharply between 1 and 3 m channel length for both brackish and seawater but then plateau at an output of 11 kg/h at about 7 m for seawater. A much flatter increase for brackish water is present as well at around 12.5 kg/h of distillate output for channel lengths above 7 m. In conclusion, a longer channel and consequently a higher membrane area do not lead to an increase in output for the same operational parameters but only to a more efficient use of heat inside the module. This is due to a reduction of transmembrane flux with decreasing ΔT driving force temperature difference as the channel is elongated.

Next, an analysis of specific electrical energy consumption SEC_{el} was undertaken since it will be a decisive factor for the economic viability in comparison with RO alongside SEC_{th} and CAPEX.

Fig. 6 shows the values SEC_{th}, SEC_{el} and over channel length at a feed mass flow rate of 300 kg/h and temperatures T_{ei} of 60 °C and T_{ci} of 10 °C. These values were used for the subsequent calculation of OPEX and CAPEX displayed in Section 4.4.

The thermal energy consumption of the MD modules reduces significantly with an increase of channel length from one to three meters; from 1098 kWh to 402 kWh per ton of produced distillate. This means that a three meter or longer channel length system requires less than half of the available heat (1000 *kWh* per ton of distillate) provided by the electrolyzer. In general, the lower salinity of the brackish water feed solution yields a higher output of distillate per kWh of thermal

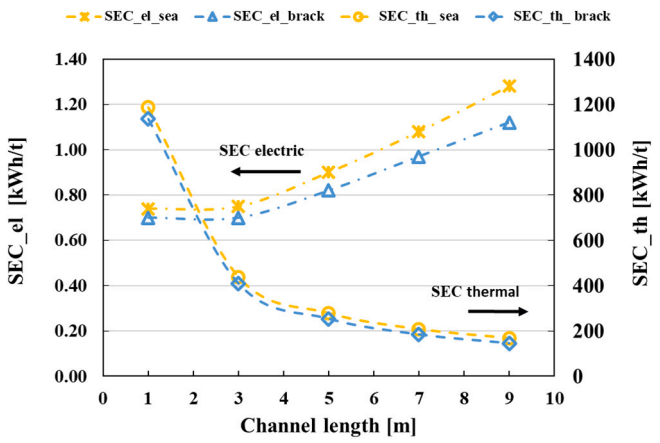

Fig. 6. SEC_{th}, SEC_{el} and for increasing MD module channel lengths; $\dot{m}_f$ = 300 kg/h, T_{ei}. = 60 °C, T_{ci}. = 10 °C, Sal = 5 (brack) and 34.3. gNaCl/kg solution (sea).

energy, resulting in the lower specific values seen in Fig. 6. The values are, however, within 5–15 % of each other across all channel lengths. On the other hand, electric energy consumption increases from 0.7 to 1.12 kWh/t for brackish and from 0.74 to 1.28 kWh/t for seawater from 1 to 9 m of channel length. Values show a linear increase with channel length, except for the 1 m channel. At this relatively short length, the pressure loss from the piping and heat exchanger is dominant compared to the pressure loss in the actual internal module channel, resulting in equal values for 1 and 3 m. For seawater desalination the specific electric energy demand is 1 to 9 % higher depending on channel length which can be explained by the same phenomenon as the lower GOR values shown in Figs. 4 and 5; a lower relative distillate output due to the impact of reduced vapour pressure in the feed results in a higher specific electrical energy consumption. Not depicted here is the impact of feed mass flow rate on the SEC_{el}. For the temperature conditions shown in Fig. 6, it varies between ~0.14–1.5 kWh/t of distillate for both salinities and feed flow rates between 100 and 400 kg/h according to the numerical calculations.

The total required membrane A_{tot} area is shown in Fig. 7 and is a defining factor for the calculation of capital costs. The required area for the targeted 1 t/h distillate capacity system increases linearly with increasing channel length from ~165 to ~850 m^2 for both brackish and seawater. Approximately 9 % more membrane is needed in the case of seawater desalination to achieve the same distillate output as a brackish

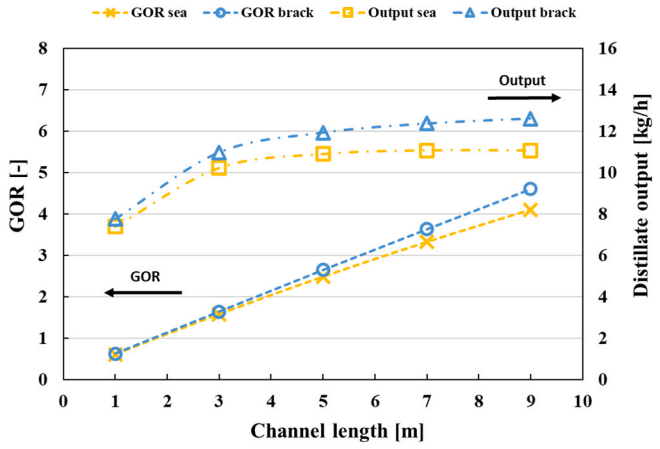

Fig. 5. GOR and MD- module channel output for increasing channel length [m] $\dot{m}_f$ = 300 kg/h, T_{ei}. = 60 °C, T_{ci}. = 10 °C; Sal = 5 (brack) and 34.3. gNaCl/kg solution (sea).

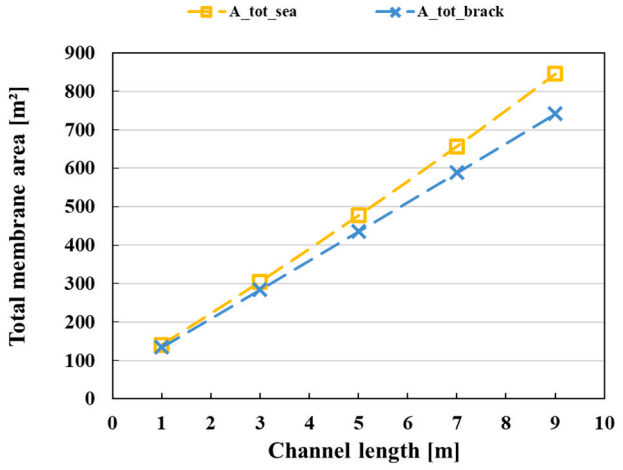

Fig. 7. Total required membrane area for a 1 t/h MD system over increasing MD module channel lengths; $\dot{m}_f$ = 300 kg/, T_{ei}. = 60 °C, T_{ci}. = 10 °C, Sal = 5 (brack) and 34.3. gNaCl/kg solution (sea).

water treatment system.

Henceforth, after analysis of thermal and electrical energy consumption and required membrane area, the economic and energy related trade-off of high efficiency against high productivity becomes more transparent for the given scenario. With respect to the results presented in Figs. 5, 6 and 7 a channel length of 3 m is expected to yield the most cost-effective system design. Selecting a shorter channel, however, comes with further considerations regarding the salinity and temperature of the retentate to be discharged from the system or further processed. It must be noted that shorter channel lengths result in a higher temperature of the concentrate discharge which can impact the surrounding ecosystems and interfere with regulatory restrictions [61].

Fig. 8 shows driving force delta T as an effect of feed inlet temperature T_{ci} (i.e., local temperature) on the evaporator outlet temperature T_{eo} (i.e., discharge temperature) for 3 m, 5 m,7 m and a 9 m MD module channel length and a feed mass flow of 300 kg/h. A difference of up to 8,5 K at an inlet temperature of 5 °C is visible between the 3 m and the 9 m channel length. The Fig. 8 represents both brackish and seawater feed since their temperature profiles are identical. A further general environmental impact of desalination technologies is the discharge outlet salinity. In comparison to SWRO with higher recovery rates of 30 %–50 %, a MD system without feed recirculation as presented in Fig. 3 has recovery ratios of around 3–4 % according to Eq. (8). On the one hand this leads to higher raw water consumption in relation to the product than RO. On the other hand, for a system without feed recirculation and a high salt rejection as demonstrated by the MD distillate quality evaluation (Section 4.1), the increase in salt concentration is minimal. For an inlet salinity of 5 and 34.3 g/kg, the maximum discharge salinity S_{eo} according to Eq. (6) is 5.2 and ~35.5 g/kg respectively.

For comparison, Table 4 provides a summary of KPIs for both brackish and feed water salinity as well as 3 m and 9 m channel lengths for a system designed for the targeted 1 t/h of distillate. Evidently, the choice of channel length has a much higher impact on the values for SEC_{th}, SEC_{el} and total required membrane area A_{tot}, than salinity. While SEC_{th} reduces from 410 kWh/t for brackish water at 3 m to 146 kWh/t at 9 m, SEC_{el} is inversely affected with more than double the amount of electricity required (0,92 kWh/t) per ton of distillate for the 9 m channel compared to 0,4 kWh/t for the 3 m channel length. Similarly, the total required membrane area A_{tot} is 2.5–2.7 times higher for the 9 m channel length systems than for those with 3 m, for brackish and seawater respectively. Assuming that 50 m^2 can be combined into one MD module, 5–6 modules are required for a 3 m channel length concept whereas 15–17 modules are required for a 9 m channel length one. Thus, the channel length selection of 3 m will be carried forward to the economic assessment within this work in Section 4.4.

Table 4
Summary of simulated KPIs for brackish and seawater desalination with MD for 3 m and 9 m channel length modules for a production of 1 t/h of distillate, $\dot{m}_f$= 300 kg/h per module, T_{ei}. = 60 °C, T_{ci}. = 10 °C.

Feed type	Channel length	SEC_th	SEC_el	A_tot	RR	Seo	No of modules k
	[m]	[kwh/t]	[kwh/t]	[m^2]	[%]	[g/kg]	[−]
Brackish water	3	410	0.4	284	3.7	5.2	5
Seawater	3	439	0.45	305	3.4	35.5	6
Brackish water	9	146	0.92	742	4.2	5.2	15
Seawater	9	169	1.1	845	3.7	35.6	17

4.3. RO system design

Water Application Value Engine software (Wave, Dupont) was used to size and simulate RO plants with the different NaCl feed solutions mentioned in the previous section. The simulations served to estimate specific electrical energy consumptions and membranes required. A 50 % recovery was selected for all designs for comparison purposes. Inlet water temperatures were varied between 5, 10 and 20 °C to match the MD simulations. The plants were sized with 2 passes with arrays of 6 membrane elements per vessel and a target product electrical conductivity of 10 µS/cm or lower.

4.4. RO performance analysis

RO plants designed to deliver pure water at 50 % recovery were simulated at the two different feed salinities of 5 and 34.3. gNaCl/kg and inlet temperatures of 5, 10 and 20 °C. The most suitable designs resulted in a two-pass plants for both brackish (brackish water membranes) and for seawater (seawater and brackish water membranes) desalination. All designs delivered product qualities between 1 and 8 µS/cm, which are on average slightly higher than the experimental values for MD (see Table 3).

Further improvements in product quality with RO or MD are not technically feasible. A polishing step to further reduce remaining ions and dissolved gases are necessary for both technologies to meet ultrapure requirements. The estimated specific energy consumptions SEC_{el} for brackish and seawater are presented in Fig. 9, where each marker represents a different inlet temperature. As expected, both parameters have an important impact in energy use for RO systems, with consumption increasing with increasing salinity and decreasing

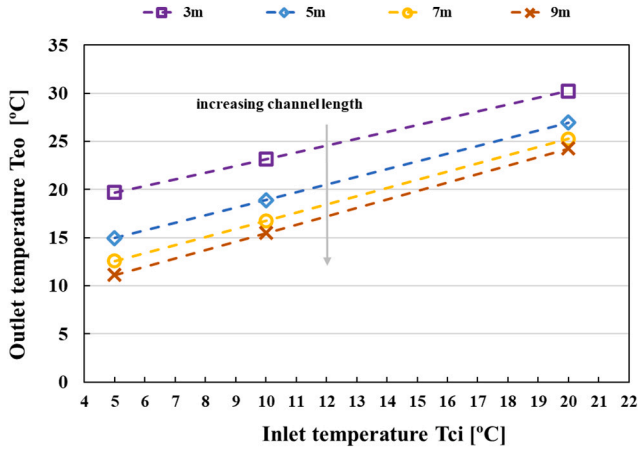

Fig. 8. Influence of feed inlet temperature T_{ci}. on evaporator outlet (discharge) temperature T_{eo}; $\dot{m}_f$= 300 kg/h; T_{ei} = 60 °C; brackish water & seawater.

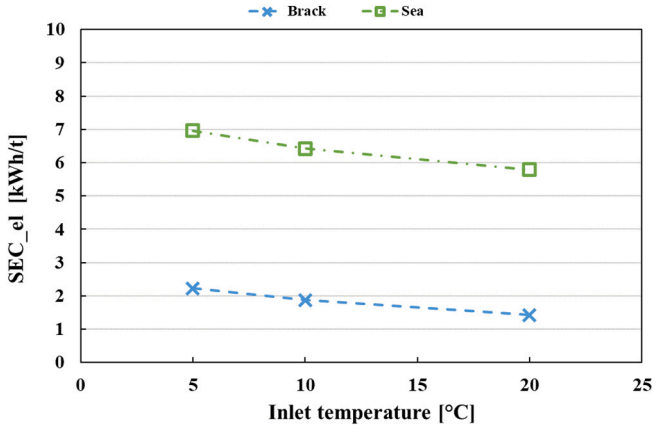

Fig. 9. Simulated specific energy consumption for brackish and seawater two-pass RO systems Sal = 0.5 (brack) and 34.3. gNaCl/kg solution (sea) at different inlet water temperatures 5,10 and 20 °C.

temperature. Specific energy consumption in the seawater desalination plant reaches 5.8 (20 °C) to 7.0 (5 °C) kWh per ton of product water, being significantly higher than for brackish water at 1.4–2.2 kWh/t respectively. These results are within the higher end range of reported values for brackish and seawater RO plants [62,63]. However, both RO plants were designed in the current study with two passes to increase product quality, whereas literature values typically correspond to one-pass systems. For the entire operational range of both feed solutions, the SEC_e values for RO largely exceed those for MD. Given the pressure driven nature of the process and pumping energy required, this is to be expected.

5. Economic assessment

5.1. Cost calculation methods

Cost evaluation of the MD and RO system is conducted by separating the costs into capital expenditures (CAPEX) and operational expenditures (OPEX) and analyzing these over a fixed plant lifetime. To perform a valid comparison with RO technology, values for unit cost per cubic meter of distillate were obtained from literature for plants in a similar size range. The cost evaluation is carried out for an approximate capacity of 1 t/h distillate from feed waters of two different salinities of 5 and 34.3 gNaCl/kg and 8000 operating hours per year. The results are provided in the currency Euros.

5.1.1. MD capital costs

For MD, capital costs accrue from MD modules, piping, electrics, sensors, instrumentation, design and finally the installation costs onsite. The annually amortized capital expenditures a_{AMOR} are derived from the total capital investment costs C_I with assumed interest rates i of 4 % and 6 % over a lifetime n of 20 years as calculated in Eq. (10).

$$a_{AMOR} = C_I \left[\frac{i\,(1+i)^n}{(1+i)^n - 1} \right] \; [€] \tag{10}$$

Interest rates have been selected based on the interest rates in the countries in the EU around the North and Baltic Sea with the highest probability of offshore production of Hydrogen. This includes Germany, The Netherlands, Denmark, Sweden, Poland, Norway, Lithuania, Latvia, Finland and Estonia. The lower interest rate of 4 % represents the rounded average rate of Germany in the past two years [64] and the higher interest rate of 6 % is the average rate of Poland in the last two years [64]. The interest rates of the other countries in question lie within that spread.

A further breakdown of the capital costs is done by differentiating between membrane specific module costs C_{MOD} (€ /m^2) and module specific rest of plant costs C_{ROP} *(€ /no. of modules)*. Membrane specific module costs [30] have been previously evaluated depending on the necessary membrane area A_{tot}. However, within this work, due to the advancements in MD module production technology, they will be set at 100 €/m^2. As with [30], one MD module is assumed to have a membrane surface of 50 m^2 and the rest of plant costs including pumps, heat exchangers, sensors, piping, and the pretreatment unit have been estimated in dependency of the number of modules.

The required surface area is estimated in Eq. (11) depending on the predicted average flux j_d from the numerical model, the aimed hourly capacity $\dot{q}_{aim}$ of 1 t/h and a 5 % overdesign factor.

$$A_{tot} = \frac{\dot{q}_{aim}}{jd} 1.05 \; [m^2] \tag{11}$$

From the resulting surface area, the number of modules required is calculated as.

$$k = \frac{A_{tot}}{50} \; [m^2] \tag{12}$$

which also determines the upscaled feed volume flow F_e.

$$C_I\,[30] = C_{MOD}\,A + C_{ROP}\,k\;[€] \tag{13}$$

Eq. (13) shows the calculation of the capital costs for MD units according to [30]. However, since the costs in [30] were determined in the year 2017, a cost increase due to inflation must urgently be considered. The chemical engineering plant cost index CEPCI [65] was therefore applied to adapt the values of C_I [30]. Eq. (14) represents the exemplary calculation for C_I [30].

$$C_I = C_I\,[30]\,\frac{Cost\ Index_{2023}}{Cost\ Index_{2017}}\;[€] \tag{14}$$

The latest cost index from the year 2023 equals 800.8. The reference cost index from the year 2017 is 567.5 [65]. A further 20 % of installation costs are added to the inflation adjusted value of C_I from Eq. (14). For a brackish water MD system C_I amounts to 97,605 € and to 103,306 € for a seawater system.

5.1.2. RO capital cost

Reverse osmosis desalination systems with capacities in the range of a few tons (i.e. few cubic meters) per hour can be considered small-scale plants. Information on such plants is somewhat limited in literature as most estimations or actual data is available for applications at larger scale. Unit capital costs of RO desalination plants at different capacities can be found with [66]. It was reported that plants under 10,000 t/d cost around 1000 US$ per t/d. Unit costs can be even higher at 2500 US$ per t/d for 200-t/d plants. A study [67] on different water treatment pathways for hydrogen production described investment costs of 575,000 € for a seawater RO plant with 700-t/d capacity. Costs for small-scale (5 t/h) 2-pass brackish water RO systems with an integrated electrodeionization were also reported at around 245,000 € [24]. Furthermore, capital costs for RO plants may largely vary depending on the quality of the raw water, particularly its dissolved ion content. In waters with high TDS such as seawater, more than one pass may be needed to reach relatively pure permeate along with additional equipment—i.e., corrosion-resistant piping, vessels, high-capacity pumps.

Due to these complexities and the particularities, a conservative investment cost of 175,000 € was chosen for the RO plants with a capacity of 1 t/h processing waters with 5 and 34.3 gNaCl/kg solution. These costs include RO modules, installation, piping, sensors, instrumentation, and design, while excluding any intake equipment, pre- and post-treatment processes as for the MD cost estimations. Capital costs for the RO plants were amortized for a total of 20 years as described by Eq. (10) in the previous section.

5.1.3. Operating and unit costs for MD and RO

Operating expenditure refers to the annual continuous costs resulting from the operation of the system. It is separated into the following categories.

- Thermal energy (only for MD)
- Electrical energy
- Chemicals
- Labor
- Replacement
- Insurance
- Service and maintenance

In this study the thermal energy utilized of the MD system is assumed to be readily available as presented in Section 4.1 and free of cost since the electrolyzer needs to be cooled continuously during operation. For this reason, the components and hardware required to harness and transfer the waste heat shown in the upper dotted box of Fig. 3 are considered as cost neutral.

The electrical energy demand is mainly dependent on the specific energy consumption of the pumps, taking into account the flow rate of

the feed channels and resulting pressure loss. The annual electrical costs a_{el} are estimated with a variable unit price for electricity p_{el} and the yearly distillate capacity $\dot{q}_d$ in Eq. (15). Cost evaluations are made for electrical unit prices of 0.10 and 0.40 €/kWh [69] with the aim of representing a broad spectrum of costs for industrial electricity used globally.

$$a_{el} = \dot{q}_d \, SEC_{el} \, p_{el} \tag{15}$$

Expenses for chemicals are estimated to be 0.01 $€/m^3$of feed water [23]. The feed water itself comes at a cost of 0.001 $€/m^3$.

The required labor to operate and supervise a fully automatic desalination plant has been estimated to be one full operator for a system capacity of 1000 t/day of distillate. Hydrogen electrolyzer plants of >100 MW_{el} would require several of the presented plants operating in parallel, which could be monitored by one operator. The annual costs of labor a_l proportional to the capacity of the plant $\dot{q}_d$ is calculated in Eq. (16) together with scalability factor of 0.002 [23] at an annual salary of 45 000 €.

$$a_l = \left(0.002 \frac{\dot{q}_d}{365}\right) 45000€ \Big/ \text{year} \tag{16}$$

The yearly cost of replacement of MD modules a_{REP} presented in Eq. (17) significantly defines the OPEX. Since MD is less susceptible to blocking than RO, the lifetime of MD modules n_{MOD} is assumed to be five years [69]. Each replacement y for $0 < y\, n_{MOD} < n$ happens inconsistently throughout the lifetime. To have a comparable net present value for each year, the sum of each replacement y is converted by multiplication with the amortization factor into annual charges. Parts of the modules are reusable. Therefore, the replacement costs are estimated at 80 % of the original module costs [23].

$$a_{rep} = \left[\frac{i\,(1+i)^n}{(1+i)^n - 1}\right] \sum_y \left(\frac{0.8\, C_{MOD}}{(1+i)^{y \bullet n_{MOD}}}\right) \tag{17}$$

For the case of the replacement of RO membranes, undiscounted unit costs per membrane were assumed at 500 € for seawater and 400 € for brackish water modules. Additionally, a lifetime was defined of 7 and 10 years for seawater and brackish membranes, respectively, and distributed as running annual costs [70].

The insurance costs a_{in} is calculated to be 0.5 % while service and maintenance a_{SM} are estimated at 2.5 % of the total capital investment costs for both MD and RO [23] as shown in Eqs. (18) and (19).

$$a_{in} = 0.005\, C_I \tag{18}$$

$$a_{SM} = 0.025\, C_I \tag{19}$$

Taking all annual charges into account the unit price for one ton of produced distillate is calculated in Eq. (20).

$$p_{unit} = \frac{a_{amor} + a_{el} + a_l + a_{rep} + a_{in} + a_{SM} + a_{chem} + a_f}{\dot{m}_d \, 8000\, h \Big/ a} \tag{20}$$

5.2. Economic comparison of desalination technologies

The following section assesses and compares the unit price as well as the annual costs for brackish water and seawater desalination by waste heat driven membrane distillation and reverse osmosis. Fig. 10 shows the unit price per ton of MD and RO for brackish water and Fig. 11 provides the corresponding values for seawater. Two different electricity prices of 0.10 Eur/kWh and 0.40 Eur/kWh as well as two interest rates of 4 % and 6 % are applied. The MD system is designed for a 3 m channel length system with a nominal feed mass flow rate of 300 kg/h and assumed to operate at a condenser inlet temperature T_{ci} of 10 °C and an evaporator inlet temperature T_{ei}. of 60 °C. Costs for the brackish and seawater RO desalination plants were based on a two-pass system

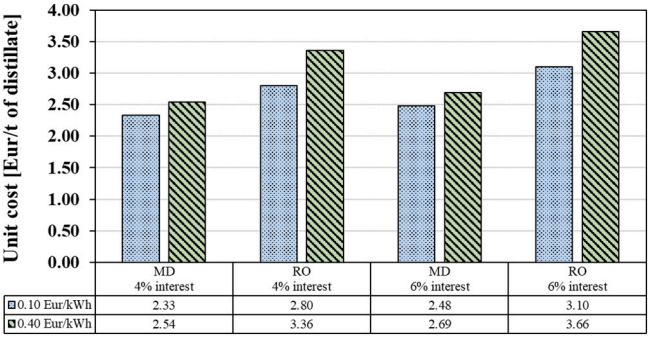

Fig. 10. Brackish water: unit price per ton of produced distillate for MD and RO with feed Sal = 5 g/kg.

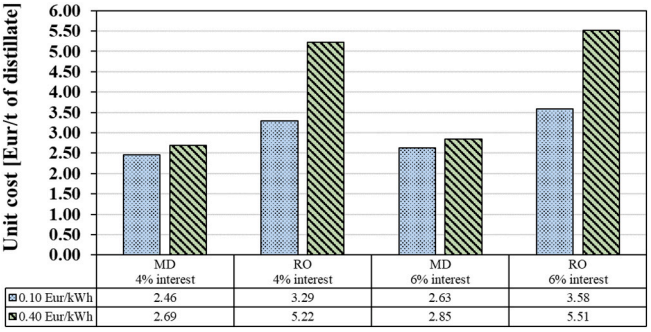

Fig. 11. Seawater: unit price per ton of produced distillate for MD and RO with feed; Sal = 34.3 g/kg.

operated at 50 % recovery and 10 °C inlet water temperature.

Overall, the unit costs with use of MD are lower than for the use of RO for both brackish and seawater desalination. While the unit costs range between 2.48 and 2.69 €/t of distillate with MD depending on electricity price at 6 % interest, they are 3.10–3.66 €/t for RO. The difference is even more pronounced for seawater desalination with unit costs of 2.63–2.85 €/t for MD and 3.58–5.51 €/t for RO at 6 % interest. For 4 % interest the unit cost for brackish water is 2.33–2.54 €/t with MD and 2.8–3.36 €/t with RO and 2.46–2.69 €/t with MD as well as 3.29–5.22 €/t of pure water with RO for seawater desalination respectively, depending on electricity costs.

Unit costs for brackish and seawater RO are higher than those of MD due to the higher capital investment costs and electrical energy consumption. As discussed in the previous section, water salinity has a direct effect on the energy consumption of RO plants. This is observed in the higher prices for seawater plants, as variations in energy prices are evident in the overall unit price. For this case, energy expenses correspond to around 18 to 52 % of the total unit price, while for brackish water it is between 6 and 25 %.

Water costs for commercial RO desalination plants have been previously reported in literature. Values vary between 0.2 and 1.8 US$/$m^3$ and 0.45 to 3.0 US$/$m^3$ for large-scale brackish and seawater desalination, respectively [63,70,71]. Moreover, specific costs per unit of plant capacity are typically higher as capacities are lower [72]. This is the case for both brackish and seawater desalination plants previously reported and can range up to 10 €/m^3 [71,73].

The potential reduction of unit cost for waste heat driven MD also aligns well with previous techno-economic analyses. The unit cost of brackish water desalination could be reduced from 4.63 to 1.6 $/$m^3$ with the use of solar energy as a heat source by introducing 60 % of waste heat according to [74]. In an assessment by [75], costs between 5.61 and 4.27 €/m^3 were determined for fuel oil burning for plant sized of 10–100 m^3/d and 5.18–3.77 €/m^3 when solar energy was used as a

heat source. And although the absolute values are considered outdated by this group of authors, both [39,76] show the potential savings through the use of waste heat with MD.

It is important to note that factors such as target product quality, energy source, temperature level and system design influence the overall costs and thus water cost values are project specific. However, the methodology followed in this study allows for a fairer analysis between MD and RO since comparable design parameters and targets are defined.

If thermal energy is assumed to be free of charge, the costs of electricity, module replacement, chemicals and labour will define the major fraction of the operating costs of the hybrid system. Fig. 12 provides an annual cost breakdown including, a_{AMOR}, *Electricity Costs* and *Other OPEX* for a mid-range electricity price of 0,25 €/kWh and 6 % interest rate. Thus, the amortized annual CAPEX a_{AMOR} for MD is 9573.00 € for a brackish water and 10,137.00 € for a seawater and 15,257,00 € for RO in both cases. Since less pumping energy is required to power the pump of the thermal driven MD systems than for the pressure driven RO systems, *Electricity Costs* are significantly higher for RO than for MD, particularly for seawater, due to the higher osmotic pressure difference across the RO membranes. While 1400.00 € and 1533.00 € incur for the brackish and seawater systems with MD, with RO 3760.00 € and 12,860,00 € must be accounted for annually to electrically power the systems. The remaining operational costs *Other OPEX* are however slightly higher for MD at 9815.00 € and 10,392.00 €, while 8023.00 € and 8274,00 € for RO for brackish and seawater. This is mainly owed to the replacement interval assumed, which is 5 years for MD in both cases, however 10 years and 7 years for brackish and seawater RO respectively. In addition, chemical costs are estimated to be about 16 times higher for MD compared to RO as a result of the significantly different recovery rates.

In summary, both unit cost and annual costs reflect the cost-efficiency of MD to produce UPW for hydrogen electrolysis if integrated for waste heat utilization. It must also be emphasized, that according to the presented analysis either most of the heat or only a portion of the available waste heat can be used by the MD system. This implies that in order to fully control operating temperatures in a PEM stack, partial cooling has to be incorporated in the balance of plant of the electrolyzer. This would also bring additional capital and operating costs to the overall MD-electrolyzer system. Furthermore, with no additional heat utilization, cooling will always be required when applying RO. This additional cost evaluation was however outside the scope of this work, since the design of said cooling system comes with a high number of individual parameters specific to the conditions on site and of the electrolysis operation.

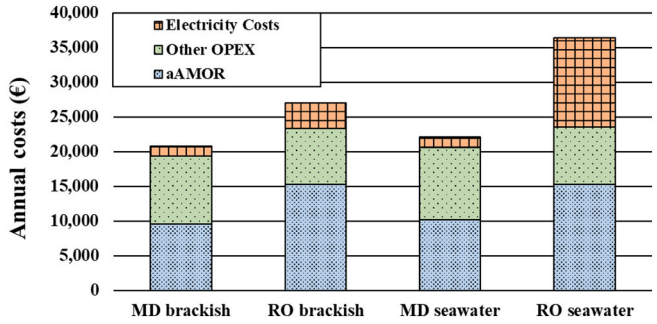

Fig. 12. Annual cost breakdown for MD and RO with brackish and seawater as feed; Electricity costs 0,25 €/kWh, Interest = 6 % p.a.

6. Conclusions

A techno-economic evaluation on the application of permeate gap membrane distillation (MD) for the production of ultrapure water for water electrolysis was carried out in this work. The assessment was based on a numerical simulation of different MD design parameters at different water salinities, considering the coupling of waste heat to supply a 5 MW PEM electrolyzer. Additionally, an experimental evaluation at laboratory scale was conducted to assess MD performance under selected conditions.

The experimental results demonstrated that MD maintained a constant production and was able to deliver high quality distillate at conductivities below 5 µS/cm regardless of feed salinity, mean temperature or temperature difference across the membrane. An evaluation of different KPIs showed the relevance of design parameters such as channel length, which largely influences energy demands and the required membrane area.

The results of the subsequent economic assessment indicated that significant cost advantages can exist with MD over reverse osmosis, considering the studied 1 t/h capacity and the utilization of waste heat from the PEM electrolyzer for thermal-driven desalination. RO exhibits higher unit costs as well as annual costs across all scenarios for brackish water and seawater feed salinities, mainly due to the significantly higher electrical energy demands and costs. Furthermore, without the need for a high GOR due to a relative abundance of heat, choosing a short channel module design of 3 m to reduce electrical energy demand as well as total membrane area led to a reduction in CAPEX and OPEX.

A topic to be addressed in more detail in the future is the conceptualization of the discharge of the brine, regardless of which feed source it is generated from. Depending on the choice of discharge strategy, having a very low recovery ratio such as with MD can be an added advantage. This can be applied to sustain a relatively low increase in salinity. Potential drawback that still remain such as temperature changes from local conditions or limited applicability of minimum or zero liquid discharge approaches.

Considering all factors, heat-integrated MD for UPW production for water electrolysis shows potential to be a breakthrough application of this technology, offering alternative desalination as well as temperature control solutions.

Declaration of competing interest

The authors declare that they have no known competing financial interests or personal relationships that could have appeared to influence the work reported in this paper.

Appendix A. Variables/parameters used in a multi node simulation model for the single MD module, values are upscaled by multiplication to achieve the target system capacity

Parameter	Symbol	Value/range	Unit
Evaporator inlet temperature	T_{ei}	60	°C
Condenser inlet temperature (feed inlet)	T_{ci}	5; 10; 20	°C
Feed mass flow rate	$\dot{m}_f$	100; 200; 300; 400	kg/h
Feed salinity at inlet	S_{ci}	5; 34.3	gNaCl/kg
Channel length	L	1; 3; 5; 7; 9	m
Membrane thickness	δ_M	70	µm
Backing thickness	δ_B	254	µm
Channel width of evaporator and condenser	$\delta_{E/C}$	2.15	mm
Permeate gap thickness	δ_{PG}	0.3	mm
Nominal pore diameter	d_M	0.2	µm
Porosity of membrane	ε_M	0.85	–
Porosity of backing	ε_B	0.55	–
Porosity of spacer evaporator and condenser channel	ε_S	0.8	–
Impermeable foil thickness	δ_F	100	µm
Feed pump efficiency	ϵ_P	75	%
Tortuosity of the membrane	τ_M	1.3	–
Height of active membrane area	h	0.5	m

References

[1] J. Töpler, J. Lehmann, Wasserstoff und Brennstoffzelle, Springer, 2014.
[2] I. R. E. Agency, Green Hydrogen Cost Reduction: Scaling up Electrolysers to Meet the 1.5°C Climate Goal, 2020.
[3] F. Mehraban, X. Tang, S. Yang, X. Wu, C. Lin, L. Tan, W. Hu, D. Zhou, J. Li, X. Li, Harnessing direct seawater electrolysis for a sustainable offshore hydrogen future: a critical review and perspective, Appl. Energy 384 (125468) (2025).
[4] H. Becker, J. Murawski, D. Shinde, I. Stephens, G. Hinds, G. Smith, Impact of impurities on water electrolysis: a review, Sustainable Energy Fuels 7 (2023) 1565–1603.
[5] Wiedenmannott, Industrielle Wasseraufbereitung - Anlagen, Verfahren, Qualitätssicherung, 1 ed., John Wiley & Sons, Inc, 2017.
[6] A. Jonsson, H. Mässgard, An Industrial Perspective on Ultrapure Water Production for Electrolysis_, 2021.
[7] F.-Y. Gao, P.-C. Yu, M.-R. Gao, Seawater electrolysis technologies for green hydrogen production: challenges and opportunities, Curr. Opin. Chem. Eng. 36 (2022) 100827.
[8] R. Yoshimura, S. Wai, Y. Ota, K. Nishioka, Y. Suzuki, Effects of Artificial River water on PEM water electrolysis performance, Catalysts 12 (2022).
[9] ASTM, "Standard Specification for Reagent Water," American Society for Testing and Materials-ASTM [Online]. Available, https://www.astm.org/d1193-99e01.html, 16 August 2017 [Accessed 29 November 2024].
[10] B. für Wirtschaft und Energie (BMWi), Die Nationale Wasserstoffstrategie, 2020.
[11] UNFCCC, The Paris Agreement - Publication, 2018.
[12] H. Lee, Y. Jin, S. Hong, Recent transitions in ultrapure water (UPW) technology: rising role of reverse osmosis (RO), Desalination 399 (2016) 185–197.
[13] R. Semiat, Energy issues in desalination processes, Environ. Sci. Technol. 42 (2008) 8193–8201.
[14] C. Fritzmann, J. Löwenberg, T. Wintgens, T. Melin, State-of-the-art of reverse osmosis desalination, Desalination 216 (2007) 1.76.
[15] Y. Soumbati, I. Bouatou, A. Abushaban, Y. Belmabkhout, M.C. Necibi, Review of membrane distillation for desalination applications: Advanced modeling, specific energy consumption, and water production cost, J. Water Process Eng. 71 (107296) (2025).
[16] E. Guillen-Burieza, E. Moritz, M. Hobisch, B. Muster-Slawitsch, Recovery of ammonia from centrate water in urban waste water treatment plants via direct contact membrane distillation: process performance in long-term pilot-scale operation, J. Membr. Sci. 667 (121161) (2023).
[17] M. Nadimi, M. Shahrooz, R. Wang, X. Yang, M. Duke, Process intensification with reactive membrane distillation: a review of hybrid and integrated processes, Desalination 573 (117182) (2024).
[18] F.S. Lima Brito, Y.A. Rocha Lebron, W. Guadagnin Moravia, L. Lange, M.C. Santos Amaral, Resource recovery from landfill leachate by two-stage of direct contact membrane distillation, Desalination 574 (117110) (2024).
[19] M. Bindels, J. Carvalho, G. Gonzales Bayona, N. Brand, B. Nelemans, Techno-economic assessment of seawater reverse osmosis (SWRO) brine treatment with air gap membrane distillation (AGMD), Desalination 489 (114532) (2020).
[20] M. Gulied, S. Zavahir, T. Elmakki, H. Park, G. Hijos Gago, H. Kyong Shon, D. Suk Han, Efficient lithium recovery from simulated brine using a hybrid system: direct contact membrane distillation (DCMD) and electrically switched ion exchange (ESIX), Desalination 572 (117127) (2024).
[21] R.L. Ramos, V. Moreira, Y. Lebron, M. Martins, L. Santos, M. Amaral, Direct contact membrane distillation for surface water treatment and phenolic compounds retention: from bench to pilot scale, Desalination 574 (117225) (2024).
[22] A. Deshmukh, C. Boo, V. Karanikola, S. Lin, A.P. Straub, T. Tong, D.M. Warsinger, M. Elimelech, Membrane distillation at the water-energy nexus: limits, opportunities, and challenges, Energ. Environ. Sci. 11 (5) (2018) 1177–1196.
[23] D. Winter, Membrane Distillation - A Thermodynamic, Technological and Economic Analysis, 2014.
[24] A. Jonsson, H. Mässgard, An Industrial Perspective on Ultrapure Water Production for Electrolysis, KTH Royal Institute of Technology, Stockholm, 2021.
[25] T. Arthur, G. Millar, J. Love, Thermal management of water electrolysis using membrane distillation to produce pure water for hydrogen production, J. Water Process. Eng. 67 (106255) (2024).
[26] W. Zhao, C. Quist-Jensen, Z. Zhong, N. Li, S. Araya, A. Ali, V. Liso, Membrane distillation for producing ultra-pure water for PEM electrolysis, Int. J. Hydrogen Energy 99 (2025) 232–240.
[27] C. Nellessen, T. Klein, H.-J. Rapp, F. Rögener, Klimaschonung durch Membrananwendung – Membrandestillation zur Erzeugung von pharmazeutischem Reinstwasser, Chem. Ing. Tech. 93 (2021) 1345–1351.
[28] J. van Medevoort, N. Kuipers, P. ten Hoopen, Hydrogen from Seawater Via Membrane Distillation and Polymer Electrolyte Membrane Water Electrolysis, 2022.
[29] T. Arthur, G. Millar, J. Love, Integration of waste heat recovered from water electrolysis to desalinate feedwater with membrane distillation, *J. Water* Process Eng. no. 56 (2023) 104426.
[30] R. Schwantes, K. Chavan, D. Winter, C. Felsmann, J. Pfafferott, Techno-economic comparison of membrane distillation and MVC in a zero liquid discharge application, Desalination 428 (2018) 50–68.
[31] L. Francis, F.E. Ahmed, N. Hilal, Advances in membrane distillation module configurations, Membranes no. 81 (2022).
[32] A. Ali, M. Shirazi, L. Nthunya, R. Castro-Munoz, N. Ismail, N. Tavajohi, G. Zaragoza, C. Quist-Jennsen, Progress in module design for membrane distillation, Desalination 581 (2024) 117584.
[33] A. Alkhudhiri, N. Darwish, N. Hilal, Membrane distillation: a comprehensive review, Desalination 287 (2012) 2–18.
[34] D. Winter, J. Koschikowski, M. Wieghaus, Desalination using membrane distillation: experimental studies on full scale spiral wound modules, J. Membr. Sci. 375 (2011) 104–112.
[35] A. Hagedorn, G. Fieg, D. Winter, J. Koschikowski, T. Mann, Methodical design and operation of membrane distillation plants for desalination, Chem. Eng. Res. Des. 125 (2017) 265–281.
[36] R. Schwantes, A. Cipollina, F. Gross, J. Koschikowski, D. Pfeifle, M. Rolletschek, V. Subiela, Membrane distillation: solar and waste heat driven demonstration plants for desalination, Desalination 323 (2013) 93–106.
[37] A.M. Alklaibi, N. Lior, Membrane-distillation desalination: Status and potential, Desalination 171 (2005) 111–131.
[38] K.W. Lawson, D.R. Lloyd, Membrane distillation. II. Direct contact MD, J. Membr. Sci. 120 (1996) 123–133.
[39] S. Al-Obaidani, E. Curcio, F. Macedonio, G.D. Profio, H. Al-Hinai, E. Drioli, Potential of membrane distillation in seawater desalination: thermal efficiency, sensitivity study and cost estimation, J. Membr. Sci. 323 (2008) 85–98.
[40] M. Gryta, Osmotic MD and other membrane variants, J. Membr. Sci. 246 (2004) 145–156.
[41] L. Zhang, M. El-Rady Abu-Zeid, Y. Zhang, H. Dong, H.-L. Chen, L. Hou, A comprehensive review of vacuum membrane distillation technique, Desalination 356 (2015) 1–14.
[42] I. Requena, J. Andres-Manas, G. Zaragoza, Influence of internal design on the performance of pilot vacuum-assisted air-gap membrane distillation modules for brine concentration with solar energy, Desalination 573 (117218) (2024).

[43] Y. Suga, R. Takagi, H. Matsuyama, Effect of the characteristic properties of membrane on long-term stability in the vacuum membrane distillation process, Membranes MDPI 11 (4) (252) (2021).
[44] VDI-Warmeatlas 11, Auflage, Springer, Berlin, 2013.
[45] AirLiquide, 2021.
[46] B. Emonts, M. Müller, M. Hehemann, H. Janßen, R. Keller, M. Stähler, A. Stähler, V. Hagenmeyer, R. Dittmeyer, P. Pfeifer, S. Waczowicz, M. Rubin, N. Munzke, S. Kasselmann, A holistic consideration of megawatt electrolysis as a key component of sector coupling, Energies 15 (2022).
[47] M. Ni, M.K.H. Leung, D.Y.C. Leung, Energy and exergy analysis of hydrogen production by a proton exchange membrane (PEM) electrolyzer plant, Energ. Conver. Manage. 49 (2008) 2748–2756.
[48] E. van der Roest, R. Bol, T. Fens, A. van Wijk, Utilisation of waste heat from PEM electrolysers – unlocking local optimisation, Int. J. Hydrogen Energy 48 (72) (2023) 27872–27891.
[49] T. Maeda, H. Ito, Y. Hasegawa, Z. Zhou, M. Ishida, Study on control method of the stand-alone direct-coupling photovoltaic – water electrolyzer, Int. J. Hydrogen Energy 37 (2012) 4819–4828.
[50] M. Espinosa-López, C. Darras, P. Poggi, R. Glises, P. Baucour, A. Rakotondrainibe, S. Besse, P. Serre-Combe, Modelling and experimental validation of a 46 kW PEM high pressure water electrolyzer, Renew. Energy 119 (2018) 160–173.
[51] W.J. Tiktak, Heat Management of PEM Electrolysis, a Study on the Potential of Excess Heat from Medium- to Large-Scale PEM Electrolysis and the Performance Analysis of a Dedicated Coling System, 2019.
[52] F. Scheepers, M. Stähler, A. Stähler, E. Rauls, M. Müller, M. Carmo, W. Lehnert, Temperature optimization for improving polymer electrolyte membrane-water electrolysis system efficiency, Appl. Energy 283 (2021) 116270.
[53] R. Gustavson, S. Hiibel, A. Childress, Membrane distillation driven by intermittent and variable-temperature waste heat: system arrangements for water production and heat storage, Desalination 448 (2018) 48–59.
[54] B. f. S. u. Hydrographie, State of the North Sea [Online]. Available, https://www.bsh.de/EN/TOPICS/Monitoring_systems/State_of_the_North_Sea/state_of_the_north_sea_node.html [Accessed 12 November 2024].
[55] M. Matheswaran, T.O. Kwon, J. Kim, M. Duke, S. Grey, I. Moon, Effects of operating parameters on permeation flux for desalination of sodium, Desalin. Water Treat. 13 (2010) 362–368.
[56] A. Ruiz-Aguirre, J.A. Andrés-Mañas, J.M. Fernández-Sevilla, G. Zaragoza, Modeling and optimization of a commercial permeate gap spiral wound membrane distillation module for seawater desalination, Desalination 419 (2017) 160–168.
[57] D. Winter, J. Koschikowski, F. Gross, M. Maucher, D. Düver, M. Jositz, T. Mann, Comparative analysis of full-scale membrane distillation contactors -methods and modules, J. Membr. Sci. 524 (2017) 758–771.
[58] R. Schwantes, L. Bauer, K. Chavan, D. Dücker, C. Felsmann, J. Pfafferott, Air gap membrane distillation for hypersaline brine concentration: operational analysis of a full-scale module–new strategies for wetting mitigation, Desalination 444 (2018) 13–25.
[59] J. Gil, A. Ruiz-Aguirre, L. Roca, G. Zaragoza, M. Berenguel, Prediction models to analyse the performance of a commercial-scale membrane distillation unit for desalting brines from RO plants, Desalination 445 (2018) 15–28.
[60] A. Ruiz-Aguirre, A. Andres-Manas, J. Fernandez-Sevilla, G. Zaragoza, Experimental characterization and optimization of multi-channel spiral wound air gap membrane distillation modules for seawater desalination, Sep. Purif. Technol. 205 (2018) 212–222.
[61] S. Lattemann, T. Höpner, Environmental impact and impact assessment of seawater desalination, Desalination 220 (2008) 1–15.
[62] T. Mezher, H. Fath, Z. Abbas, A. Khaled, Techno-economic assessment and environmental impacts of desalination technologies, Desalination 266 (2011) 263–273.
[63] D. Curto, V. Franzitta, A. Guercio, A review of the water desalination technologies, Appl. Sci. 11 (2021).
[64] E. Commission, Reference and discount rates (in %) since 01.08.1997 [Online]. Available, https://competition-policy.ec.europa.eu/state-aid/legislation/reference-discount-rates-and-recovery-interest-rates/reference-and-discount-rates_en [Accessed January 2025].
[65] T. U. o. Manchester, Chemical Engineering Plant Cost Index [Online]. Available, https://www.training.itservices.manchester.ac.uk/public/gced/CEPCI.html?reactors/CEPCI/index.html [Accessed 16 12 2024].
[66] A.K. Plappally, V. John, H. Lienhard, Costs for water supply, treatment, end-use and reclamation, Des. Water Treatment 51 (2013) 200–232.
[67] S. Simoes, J. Catarino, A. Picado, T. Lopes, S. di Berardino, F. Amorim, F. Girio, C. Rangel, T. Ponce de Leao, Water availability and water usage solutions for electrolysis in hydrogen production, J. Clean. Prod. 315 (128124) (2021).
[69] K. Tarnacki, M. Meneses, T. Melin, J. van Medevoort, A. Jansen, Environmental assessment of desalination processes: reverse osmosis and Memstill®, Desalination 296 (2012) 69–80.
[70] N. Voutchkov, Desalination Project Cost Estimating and Management, Boca Raton, CRC Press, USA, 2019.
[71] N. Ghaffour, T. Missimer, G. Amy, Technical review and evaluation of the economics of water desalination: current and future challenges for better water supply sustainability, Desalination 309 (2013) 197–207.
[72] A. Al-Karaghouli, L. Kazmerski, Energy consumption and water production cost of conventional and renewable-energy-powered desalination processes, Renew. Sustain. Energy Rev. 24 (2013) 343–356.
[73] K. Zotalis, E. Dialyneas, N. Mamassis, A. Angelakis, Desalination technologies: hellenic experience, MDPI water 6 (5) (2014) 1134–1150.
[74] H. Usman, K. Touati, M.S. Rahaman, An economic evaluation of renewable energy-powered membrane distillation for desalination of brackish water, Renew. Energy 169 (2021) 1294–1304.
[75] D. Amaya-Vias, J. Lopez-Ramirez, Techno-economic assessment of air and water gap membrane distillation for seawater desalination under different heat source scenarios, MDPI Water no. 11 (10) (2019).
[76] U. Kesieme, N. Milne, H. Aral, C. Cheng, M. Duke, Economic analysis of desalination technologies in the context of carbon pricing, and opportunities for membrane distillation, Desalination 232 (2013) 66–74.